Technical University of Denmark

DTU

Insulators containing CuCl4X22- (X=H2O, NH3) units: Origin of the orthorhombic distortion observed only for CuCl4(H2O)22-

García-Fernández, P.; García Lastra, Juan Maria; Trueba, A.; Barriuso, M. T.; Aramburu, J. A.; Moreno, M.

Link back to DTU Orbit

DTU Library
Technical Information Center of Denmark

Insulators containing $CuCl_4X_2^{2-}$ ($X = H_2O$, NH_3) units: Origin of the orthorhombic distortion observed only for $CuCl_4(H_2O)_2^{2-}$

P. García-Fernández,[1,*] J. M. García-Lastra,[2] A. Trueba,[1] M. T. Barriuso,[3] J. A. Aramburu,[1] and M. Moreno[1]

[1]*Departamento de Ciencias de la Tierra y Física de la Materia Condensada, Universidad de Cantabria, Avenida de los Castros s/n, 39005 Santander, Spain*

[2]*Center for Atomic-Scale Materials Design, Department of Physics, Technical University of Denmark, DK-2800 Kongens Lyngby, Denmark*

[3]*Departamento de Física Moderna, Universidad de Cantabria, Avenida de los Castros s/n, 39005 Santander, Spain*

The origin of the difference in structure between compounds containing $CuCl_4X_2^{2-}$ ($X = H_2O$, NH_3) units is analyzed by means of first-principles calculations. While NH_3-containing compounds display tetragonal symmetry, H_2O-containing ones display an orthorhombic distortion at low temperature where the equatorial Cl^- ions are no longer equivalent. Our simulations of optical and vibrational transitions show good agreement with all available experimental optical absorption and Raman data. As a salient feature, the value of the force constant for the B_{1g} mode, $K(B_{1g})$, driving the orthorhombic distortion in the $CuCl_4(H_2O)_2^{2-}$ unit is found to be four times smaller than that calculated for $CuCl_4(NH_3)_2^{2-}$, stressing that $CuCl_4(H_2O)_2^{2-}$ is in the verge of the $D_{4h} \rightarrow D_{2h}$ instability. The analysis of results obtained for different values of the distortion coordinate, $Q(B_{1g})$, clearly shows that the softening undergone by $K(B_{1g})$ in $CuCl_4(H_2O)_2^{2-}$ comes mainly from the vibronic admixture of the antibonding $a_{1g}^*(\sim 3z^2$-$r^2)$ orbital with the b_{1g}^b bonding (or charge transfer) level. This mechanism is thus similar to that responsible for distortions observed in some fluoroperovskites and oxoperovskites. The present results, quantifying the importance of vibronic effects in structural instabilities, clearly demonstrate that, contrary to what was suggested by several authors, the instability in $CuCl_4(H_2O)_2^{2-}$ is not related to the Jahn-Teller effect and that the orthorhombic distortion observed in the pure compound $Rb_2CuCl_4(H_2O)_2$ has a local origin.

PACS number(s): 64.60.an, 71.70.Ej, 61.72.Bb, 31.15.ae

I. INTRODUCTION

It is well-known that compounds that are rather similar from a chemical point of view can exhibit a different structure at low temperatures and thus distinct physicochemical properties. This situation is found when studying, for example, the series of oxoperovskites $ATiO_3$ ($A = Ca^{2+}$, Sr^{2+}, Ba^{2+}), where the three crystals display a cubic phase at high temperatures, but at lower ones their behavior differs considerably. $SrTiO_3$ is cubic down to 105 K, where it becomes slightly tetragonal due to the rotation along the z axis of the TiO_6 octahedra.[1,2] On the other hand, $CaTiO_3$ presents much stronger rotations around all cartesian axes becoming orthorhombic below 1580 K[3] and, finally, $BaTiO_3$, while not presenting octahedral rotations, becomes ferroelectric running through a tetragonal, an orthorhombic, and a rhombohedral phase as the temperature lowers.[4,5] Similarly, the different occupations of the $3d$-orbitals in $KNiF_3$ and $KMnF_3$ lead $KNiF_3$ to be cubic at all temperatures, while $KMnF_3$ presents octahedral rotations at low temperature like in $CaTiO_3$.[6,7] These phase transitions arise from the existence of a structural instability, a subtle phenomenon whose microscopic origin is often not well understood in detail.

In the realm of pure and doped insulators containing Cu^{2+} ions a conspicuous example of structural instability is provided by the comparison of systems containing the $CuCl_4(NH_3)_2^{2-}$ and $CuCl_4(H_2O)_2^{2-}$ units.[8–20] The $CuCl_4(NH_3)_2^{2-}$ unit is involved in the pure $CuCl_2(NH_3)_2$ crystal,[8] and it is formed as an impurity center in $HgCl_2(NH_3)_2$:Cu^{2+}[16] and in NH_4Cl:Cu^{2+} crystals grown in solution with a pH $\geqslant$ 7[9,10,12,13] (Fig. 1). This center is also formed in crystals of $CsCl$:Cu^{2+} adding ammonia to the growth solution.[9] The water-containing unit $CuCl_4(H_2O)_2^{2-}$ is also formed in NH_4Cl:Cu^{2+} crystals grown in solution but with an acidic pH (Fig. 1)[9,10,12] and is also present in pure compounds like $Rb_2CuCl_4(H_2O)_2$.[20,21] It should be noted that in this compound two neighboring $CuCl_4(H_2O)_2^{2-}$ units are actually well separated, and no ligand is shared by them.[20] This situation is thus similar to that of NH_4Cl crystals containing *isolated* $CuCl_4(H_2O)_2^{2-}$ impurity centers.

Experimental results on systems containing the $CuCl_4(NH_3)_2^{2-}$ unit are consistent for all temperatures with a tetragonal (D_{4h}) symmetry where the equatorial Cl^- ligands are all lying at the same distance, R_{eq}, from Cu^{2+}. In particular, x-ray diffraction data carried out for $CuCl_2(NH_3)_2$ give $R_{eq} = 2.76$ Å, while the Cu^{2+}-N distance, $R_{ax} = 1.96$ Å, is certainly smaller than R_{eq}.[8] Along this line, in the case of the $CuCl_4(NH_3)_2^{2-}$ center in NH_4Cl:Cu^{2+} the two A_{1g} frequencies related to the symmetric $Cu^{2+} \leftarrow NH_3$ and $Cu^{2+} \leftarrow Cl^-$ vibrations have been measured by Raman spectroscopy.[15] The experimental values $\hbar\omega(A_{1g}; Cu^{2+} \leftarrow NH_3) = 460$ cm^{-1} and $\hbar\omega(A_{1g}; Cu^{2+} \leftarrow Cl^-) = 165$ cm^{-1} measured at 100 K support that bonding in the equatorial plane is certainly much weaker that along the C_4 axis. In contrast, the low-temperature equilibrium geometry for systems with $CuCl_4(H_2O)_2^{2-}$ units is found to be not tetragonal but orthorhombic with two equatorial Cl^- ligands lying at a short distance, R_{eq}^s, and the two other lying at a longer distance, R_{eq}^l. In the case of $Rb_2CuCl_4(H_2O)_2$, the values $R_{eq}^s = 2.26$ Å and $R_{eq}^l = 3.00$ Å have been derived from x-ray diffraction,[20,21] while $R_{eq}^s = 2.25 \pm 0.15$ Å and $R_{eq}^l = 2.85 \pm 0.15$ Å come from extended x-ray absorption fine-structure (EXAFS) measurements.[21]
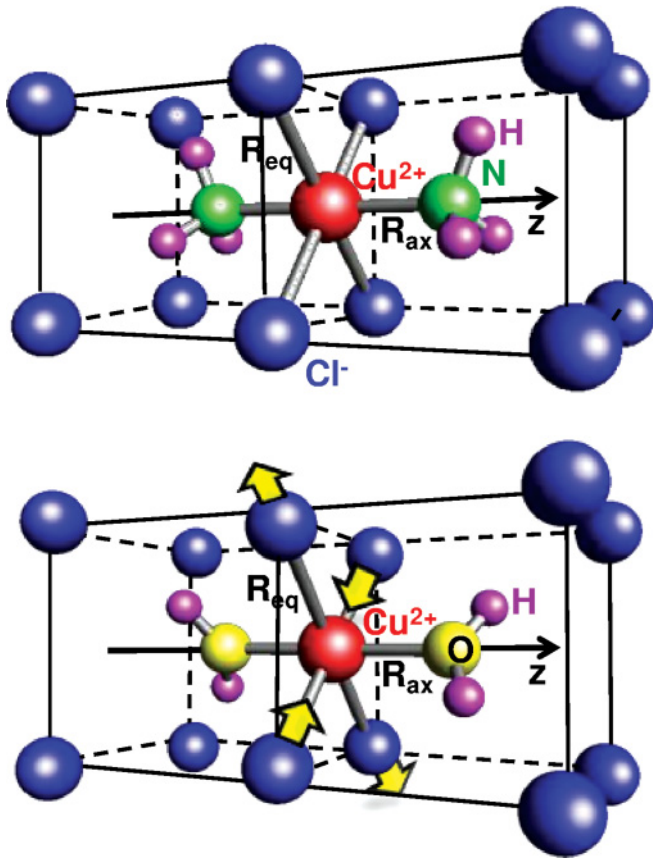
FIG. 1. (Color online) Scheme of the $CuCl_4(NH_3)_2^{2-}$ (top) and $CuCl_4(H_2O)_2^{2-}$ (bottom) centers. Cu^{2+} ion is represented by a red sphere, while Cl^- ions and N, O, and H atoms are represented, respectively, by blue (medium gray), green (gray), yellow (light gray), and small pink (light gray) spheres. In the case of the $CuCl_4(H_2O)_2^{2-}$ complex, the arrows represent the B_{1g} distortion driving the $D_{4h} \rightarrow D_{2h}$ transition at low temperatures.

The value of the Cu^{2+}-O distance is found to be $R_{ax} = 1.97$ Å,[20,21] which is practically identical to the axial distance measured for $CuCl_2(NH_3)_2$.[8]

Electron paramagnetic resonance (EPR) and electron nuclear double resonance (ENDOR) data obtained on the $CuCl_4(H_2O)_2^{2-}$ center formed in $NH_4Cl:Cu^{2+}$ are fully consistent with the existence of an orthorhombic (D_{2h}) distortion at 4.2 K involving the B_{1g} mode[10] (Fig. 1). Indeed only the superhyperfine interaction with the two closest Cl^- ligands is observed in the spectra. However, when the temperature is raised only to ~10 K, the local structure seen through EPR and ENDOR is not orthorhombic but tetragonal, a change that cannot be related to any structural phase transition of the NH_4Cl host lattice.[10] This phenomenon is thus similar to that observed in $BaF_2:Mn^{2+}$, where a $T_d \rightarrow O_h$ local phase transition is observed when the temperature is raised to about 50 K.[22–24] The existence of a $D_{2h} \rightarrow D_{4h}$ local phase transition when the temperature increases up to ~10 K for the $CuCl_4(H_2O)_2^{2-}$ center in $NH_4Cl:Cu^{2+}$ strongly suggests that the dependence of the ground-state energy on the $Q(B_{1g})$ normal coordinate should be extremely flat with two shallow minima separated by a barrier of about 10–100 cm^{-1}.

Bearing in mind all these experimental facts, it is thus challenging to shed light on the actual origin of the $D_{4h} \rightarrow D_{2h}$ instability associated with the $CuCl_4(H_2O)_2^{2-}$ unit but never observed when the $CuCl_4(NH_3)_2^{2-}$ unit is involved. It should be noticed that in some previous works such instability has been explained through a *phenomenological* E⊗e Jahn-Teller model, which introduces *extra parameters,* like an axial strain to represent the fact that the axial ligands (H_2O or NH_3) are different from the equatorial ones.[12,21] This model cannot be rigorously maintained. In particular, for the existence of the Jahn-Teller effect, the presence of an orbitally degenerate state at the *high-symmetry* initial configuration[25] is fully necessary. A cubic initial configuration holds for Cu^{2+}-doped cubic halides, but it is hard to imagine that it also happens in the case of $CuCl_4X_2^{2-}$ units ($X =$ NH_3, H_2O) because axial and equatorial ligands are certainly very different. Moreover, in the case of d^9 impurities (Cu^{2+}, Ag^{2+}, or Ni^+) in cubic halides, there is always a tetragonal distortion,[26–29] while for $CuCl_4X_2^{2-}$ units ($X = NH_3$, H_2O) the orthorhombic distortion does not appear when $X = NH_3$. Therefore, the Jahn-Teller effect seems inadequate to account for the absence of the orthorhombic instability in the $CuCl_4(NH_3)_2^{2-}$ unit, and a model better adapted to the *symmetry of the systems, which is at most tetragonal,* must be sought.

Taking into account these considerations, the instability in the $CuCl_4(H_2O)_2^{2-}$ unit is likely to be related to a *softening* of the force constant corresponding to the B_{1g} mode induced by vibronic coupling with *excited* electronic states, i.e., the pseudo-Jahn-Teller effect.[25] This mechanism, whose physical interpretation is *completely* different to the Jahn-Teller effect,[25] and which is much more general than the latter, can induce distortions for *any kind* of electronic ground state and has been shown to be responsible for the $O_h \rightarrow T_d$ instability in $BaF_2:Mn^{2+}$ (Ref. 24) and the $O_h \rightarrow C_{4v}$ instability observed in Fe^+-doped $SrCl_2$ and $KTaO_3$ lattices among many other examples[30–33] It should be noted now that the distortion driven by a true Jahn-Teller effect is *not related to the softening* of a force constant, although this mechanism is responsible for distortions when the electronic ground state is an orbital singlet.

Despite this fact, the vibronic admixture of an orbitally singlet ground state with excited electronic states does not *necessarily* lead to the existence of a distorted configuration.[25] Indeed the force constant, K, of a distortion mode, Q, involves two components

$$K = K_0 - K_v. \qquad (1)$$

Here $K_0 > 0$ means the force constant calculated *keeping* the electronic density corresponding to $Q = 0$, while K_v accounts for the changes of electronic density of the electronic ground state due to the admixture with excited electronic states when the distortion coordinate Q is activated. Thus, the K_v contribution is responsible for the softening of the force constant corresponding to the electronic ground state. Obviously, although $K_v \neq 0$, the instability takes place *only if* $K_v > K_0$.

Bearing these consideration in mind, the present work is aimed at exploring the two $CuCl_4X_2^{2-}$ ($X = H_2O$, NH_3) centers formed in NH_4Cl by means of *ab initio* calculations. As a main goal, the calculations and subsequent analysis

are addressed to explain why the orthorhombic distortion is observed only when X = H$_2$O.

This work is arranged as follows. After explaining the method of calculation in Sec. II, main results obtained through the present research are shown in Sec. III. In that section we first discuss the nature of the ground and first excited states for both CuCl$_4$$X_2^{2-}$ (X = H$_2$O, NH$_3$) species, calculating the corresponding equilibrium geometry. Once it is proved that in the electronic ground state, the unpaired electron lies in the antibonding a_{1g}^*($\sim$3z^2-r^2) orbital, we examine the charge distribution in this important orbital and explore the force constants of A_{1g} and B_{1g} vibrational modes. Next, we analyze, through the present calculations, the tiny vibronic admixture of b_{1g} orbitals in a_{1g}^*($\sim$3z^2-r^2), when $Q(B_{1g}) \neq 0$, and its influence upon the softening contribution K_v. Finally, in Sec. IV some additional comments are presented.

II. COMPUTATIONAL DETAILS

The properties of the CuCl$_4$$X_2^{2-}$ (X = H$_2$O, NH$_3$) centers embedded in NH$_4$Cl have been obtained in this work by means of *ab initio* calculations. As shown by EPR and ENDOR experiments, the active electrons of the impurity are strongly localized in the CuCl$_4$$X_2^{2-}$ complex.[9,10,12,17] This fact and the strongly ionic nature of the lattice allow us to employ a cluster approach in our calculations where the complex and its close surroundings are simulated quantum mechanically and the rest of the infinite lattice is introduced in the calculation through an effective electrostatic potential of point charges obtained by a modified Evjen-Ewald scheme. Keeping in mind that no superhyperfine EPR signal coming from NH$_4^+$ ions has been detected, reducing the number of vibrational degrees of freedom, and keeping the symmetry of the cluster as high as possible to facilitate interpretation, these ions outside the complex were replaced by K$^+$ ions in our simulation. Within these restrictions our results converge for clusters of 37 and 39 ions in the case of CuCl$_4$(H$_2$O)$_2^{2-}$ and CuCl$_4$(NH$_3$)$_2^{2-}$ centers, respectively.

All calculations have been performed in the standard spin-restricted and nonrelativistic Kohn-Sham formalism of the density functional theory (DFT) by means of the Amsterdam density functional (ADF) code (version 2010.01).[34] We have used the B3LYP[35] hybrid exchange-correlation functional, which provides an accurate and computationally balanced method that is able to correct the excess of covalence frequently found in Cu^{2+} compounds when using local (LDA) or semilocal (GGA) density functionals.[36] The Kohn-Sham orbitals were described using a Slater-function basis set of triple-ξ plus polarization quality for all ions and atoms in the complex and double-ξ for all ions outside of it. Geometry optimizations were carried out, including all degrees of freedom for the ions in the complex, while the external layers of the cluster were fixed to match the perfect lattice positions.

III. RESULTS AND DISCUSSION

A. Nature of the ground-state and equilibrium distances

In a first step we have calculated the equilibrium geometry of CuCl$_4$$X_2^{2-}$ (X = H$_2$O, NH$_3$) species in NH$_4$Cl for two different electronic states. In the A_{1g} state the unpaired electron

TABLE I. Calculated values of the equilibrium distances R_{ax} and R_{eq} (in Å) for both CuCl$_4$$X_2^{2-}$ (X = H$_2$O, NH$_3$) centers formed in NH$_4$Cl for the two A_{1g} and B_{1g} electronic states. In the A_{1g} states the unpaired electron lies in the antibonding a_{1g}^*($\sim$3z^2-r^2) orbital, while in B_{1g} it is placed in b_{1g}^*($\sim$x^2-y^2). The difference between the energy of B_{1g} and A_{1g} states computed at the corresponding equilibrium geometry, Δ_M, is also given. Δ_0 reflects the same energy difference but calculated at the equilibrium distance of the ground electronic state A_{1g}. Energies are in cm^{-1} units.

System	State	R_{ax}	R_{eq}	Δ_M	Δ_0
CuCl$_4$(NH$_3$)$_2^{2-}$	A_{1g}	1.95	2.77	9012	9300
	B_{1g}	2.04	2.75		
CuCl$_4$(H$_2$O)$_2^{2-}$	A_{1g}	1.93	2.70	4180	5500
	B_{1g}	2.07	2.60		

lies in the antibonding a_{1g}^*($\sim$3z^2-r^2) orbital, while in B_{1g} it resides in the planar b_{1g}^*($\sim$x^2-y^2) orbital. The equilibrium R_{ax} and R_{eq} distances found for both centers are gathered in Table I. As a salient feature we have found that A_{1g} is the ground state for both CuCl$_4$$X_2^{2-}$ (X = H$_2$O, NH$_3$) centers. It is worth noting that the g tensor measured for the CuCl$_4$(NH$_3$)$_2^{2-}$ unit in NH$_4$Cl is fully consistent with an A_{1g} as ground state, thus supporting the results of the present calculations.[9–11] Indeed the experimental g$_{||}$ $\cong$ 2 and g$_\perp$ = 2.22[9,10] values are the fingerprint of an unpaired electron residing in the a_{1g}^*($\sim$3z^2-r^2) orbital and not in the b_{1g}^*($\sim$x^2-y^2) orbital.[37]

Although there is no experimental information on the equilibrium R_{eq} and R_{ax} distances for CuCl$_4$(NH$_3$)$_2^{2-}$ embedded in NH$_4$Cl, the calculated figures R_{ax} = 1.95 Å and R_{eq} = 2.77 Å (Table I) are practically identical to those measured by x-ray diffraction for the CuCl$_2$(NH$_3$)$_2$ compound.[8] These distances are thus qualitatively consistent with an a_{1g}^*($\sim$3z^2-r^2) orbital as the highest-occupied antibonding orbital. Similarly, the average value $[R_{eq}^s + R_{eq}^l]/2$ = 2.63 Å derived from x-ray diffraction data for Rb$_2$CuCl$_4$(H$_2$O)$_2$[20,21] is not far from R_{eq} = 2.70 Å calculated for the electronic ground state of CuCl$_4$(H$_2$O)$_2^{2-}$ placed in NH$_4$Cl.

The value of the equatorial Cu^{2+}-Cl$^-$ distance, R_{eq} = 2.77 Å calculated for CuCl$_4$(NH$_3$)$_2^{2-}$ is certainly higher than the figure R_{eq} = 2.26 Å measured for the square planar CuCl$_4^{2-}$ unit, where the unpaired electron lies in the b_{1g}^*($\sim$x^2-y^2) orbital.[38] Therefore, these data together with the value R_{ax} = 1.96 Å (Table I) suggest that the Cu^{2+}-N bonds in CuCl$_4$(NH$_3$)$_2^{2-}$ are clearly stronger than the Cu^{2+}-Cl$^-$ bonds. According to Table I, a similar situation should hold for the CuCl$_4$(H$_2$O)$_2^{2-}$ unit, where the calculated metal-ligand distances for a D_{4h} unit are R_{ax} = 1.93 Å and R_{eq} = 2.70 Å. Further arguments on this important issue are provided in Sec. III.B.

Finally, in Table I we also present the calculated energy value for the vertical $A_{1g} \rightarrow B_{1g}$ excitation, denoted Δ_0, which has been measured by optical absorption spectroscopy in the case of the CuCl$_4$(NH$_3$)$_2^{2-}$ unit in NH$_4$Cl.[13] As can be seen, the calculated value reported in Table I is very close to Δ_0 = 9300 cm^{-1} measured experimentally.

It is worth noting now the differences between the present results and those corresponding to pure Jahn-Teller systems.
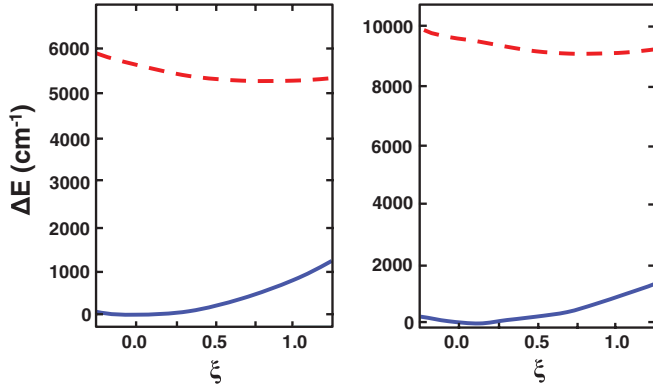
FIG. 2. (Color online) Representation of the energy surfaces along a cross-section driving the system from the A_{1g} state minimum to the B_{1g} minimum using the ξ parameter as described by Eq. (2). The solid blue and dashed red lines represent, respectively, the ground A_{1g} and excited B_{1g} states. The left plot corresponds with the water-containing unit, while the one on the right corresponds with the ammonia-containing one.

Let us designate by $E(B_{1g})$ and $E(A_{1g})$ the energies of B_{1g} and A_{1g} states and by Δ_M as the difference $E(B_{1g})$-$E(A_{1g})$ when each of the energies is computed at the stable minimum of each state. Calculated values of Δ_M are also reported in Table I, where it can be seen that $\Delta_M = 1.15$ and 0.5 eV for $CuCl_4(NH_3)_2^{2-}$ and $CuCl_4(H_2O)_2^{2-}$, respectively. Both Δ_M values are clearly higher than those obtained for d^9 impurities, which are *initially under strict octahedral coordination* but undergo a Jahn-Teller distortion.[27,39] Indeed the Δ_M values for true Jahn-Teller systems are in the range 10^{-3}–10^{-1} eV and correspond with the so called Jahn-Teller energy barrier, whose origin is the small anharmonicity naturally present in all interatomic bonds.[39,40] To further explore this point, we have calculated the variation of energy in the A_{1g} and B_{1g} states in both species as we move from an equilibrium geometry to the other varying R_{ax} and R_{eq} as follows

$$R_i = R_i(A_{1g}) + \xi[R_i(B_{1g}) - R_i(A_{1g})]$$
$$(i = eq, ax; \ 0 < \xi < 1). \tag{2}$$

As it is shown in Fig. 2, *there is no crossing of* $E(B_{1g})$ and $E(A_{1g})$ curves along this path, although in a true Jahn-Teller system, it happens for $\xi = 1/2$.[25,40] Therefore, $CuCl_4X_2^{2-}$ ($X = H_2O$, NH_3) can be viewed in principle as tetragonal species, where the distance, R_{ax}, of H_2O or NH_3 ligands to Cu^{2+} is certainly smaller than R_{eq}, and the origin of this geometry presents no clear relation to the Jahn-Teller effect.[11] Moreover, the absence of a conical intersection indicates that the Berry phase will not be present if these systems performed a pseudorotation.[25] Because the Berry phase is a clear indicator of the presence of the Jahn-Teller effect in a system, this fact further shows that the latter cannot be used to explain the origin of the distorted configuration in these systems.

B. Charge distribution in the antibonding $a_{1g}^*(\sim 3z^2-r^2)$ orbital

In the ground state of both $CuCl_4X_2^{2-}$ ($X = H_2O$, NH_3) species, the unpaired electron has been shown to lie in the $a_{1g}^*(\sim 3z^2-r^2)$ orbital. For this reason the Mulliken charge

TABLE II. Charge distribution (in %) corresponding to the antibonding $a_{1g}^*(\sim 3z^2$-$r^2)$ orbital for both $CuCl_4X_2^{2-}$ ($X = H_2O$, NH_3) centers formed in NH_4Cl. In this orbital, where the unpaired electron is placed, such an electron can be found on the $3p(Cl)$ orbitals of equatorial ligands, the $2p(N)$ or $2p(O)$ orbitals of axial ligands, as well as on the $3d(3z^2$-$r^2)$ and $4s$ orbitals of the Cu cation.

System	$3d(3z^2$-$r^2)$ Cu	$4s$(Cu)	Axial ligands	$3p$(Cl)
$CuCl_4(NH_3)_2^{2-}$	57	8	14	20
$CuCl_4(H_2O)_2^{2-}$	67	2	6	23

distribution in that orbital calculated for the ground-state geometry is displayed in Table II. We can observe in Table II that while the $3d$ (Cu) charge and the equatorial covalency are similar in both complexes, the axial covalency is rather different. For $CuCl_4(H_2O)_2^{2-}$ center, both the mixing with $O(2p)$ functions (6%) and $3d(3z^2$-$r^2)$-$4s$ hybridization in Cu [2% $4s$(Cu)] are relatively small when compared to the corresponding values in $CuCl_4(NH_3)_2^{2-}$, where the hybridization with axial $2p(N)$ and the $3d(3z^2$-$r^2)$-$4s$ hybridization are twice and four times the ones found in the previous complex. The origin of this difference lies in the fact that NH_3 is a stronger ligand than H_2O and, as a consequence, disrupts the bonding toward the axial direction more efficiently. The higher covalency induced by NH_3 as ligand when compared to that of H_2O is well reflected in both the optical electronegativity and nephelauxetic series by Jørgensen.[41]

With regard to the values collected in Table II, it should be noted that in a previous MS-Xα calculation, the amount of $4s$(Cu) in the a_{1g}^* orbital of $CuCl_4(NH_3)_2^{2-}$ was calculated to be 9%.[19] Moreover, the experimental values of the hyperfine tensor for $CuCl_4X_2^{2-}$ ($X = H_2O$, NH_3) centers in NH_4Cl[9,10,17] strongly support a much higher amount of $4s$(Cu) in the a_{1g}^* orbital for $CuCl_4(NH_3)_2^{2-}$ than for $CuCl_4(H_2O)_2^{2-}$ in agreement with results in Table II. In this sense the A_{zz} component of the hyperfine tensor, measured at 4.2 K when the magnetic field is parallel to the C_4 axis, is $A_{zz} = 726$ MHz for $CuCl_4(NH_3)_2^{2-}$, while a much smaller value $A_{zz} = 143$ MHz has been recorded for $CuCl_4(H_2O)_2^{2-}$.[10]

C. A_{1g} and B_{1g} frequencies for $CuCl_4X_2^{2-}$ ($X = H_2O$, NH_3)

Seeking to provide further insight into the origin of the different structural properties of $CuCl_4X_2^{2-}$ ($X = H_2O$, NH_3) units at low temperature, we now proceed to explore the characteristics of some representative vibrational modes.

Values of the calculated force constants and associated frequencies for relevant vibration modes of D_{4h} $CuCl_4X_2^{2-}$ ($X = H_2O$, NH_3) species in NH_4Cl are collected in Table III. In addition to results for the two symmetric Cu^{2+}-X and Cu^{2+}-Cl modes, data concerning the force constant of the distortion B_{1g} mode for both $CuCl_4(NH_3)_2^{2-}$ and $CuCl_4(H_2O)_2^{2-}$ centers are also shown in Table III. All these results correspond to the electronic ground state. For comparison purposes experimental values of the frequencies and force constants of some relevant modes of the square planar $CuCl_4^{2-}$ unit[41] are given in Table IV. Aside from the values corresponding to the A_{1g} and B_{1g} stretching modes, the frequency of the B_{2g} bending mode is also included in Table IV together with the figures obtained

TABLE III. Force constants K (in eV/Å^2) and associated frequencies $\hbar\omega$ (in cm^{-1}) corresponding to A_{1g} and B_{1g} vibrational modes calculated for the electronic ground state of CuCl$_4$X$_2^{2-}$ ($X = $ H$_2$O, NH$_3$) centers formed in NH$_4$Cl assuming a tetragonal symmetry. Experimental values of A_{1g} frequencies measured for CuCl$_4$(NH$_3$)$_2^{2-}$ in NH$_4$Cl (taken from Ref. [15]) are also given together with the calculated R_{ax} and R_{eq} distances (in Å) at equilibrium.

System	R_{ax}	R_{eq}	Mode	K	$\hbar\omega$ Calculated	$\hbar\omega$ Experim.
CuCl$_4$(NH$_3$)$_2^{2-}$	1.96	2.78	A_{1g}(Cu-NH$_3$)	13.4	460	460
			A_{1g}(Cu-Cl)	3.6	165	165
			B_{1g}(Cu-Cl)	1.3	99	–
CuCl$_4$(H$_2$O)$_2^{2-}$	1.94	2.70	A_{1g}(Cu-H$_2$O)	10.9	404	–
			A_{1g}(Cu-Cl)	3.44	162	–
			B_{1g}(Cu-Cl)	0.3	49	–

for the O$_h$ CrCl$_6^{3-}$ unit formed in Cs$_2$NaScCl$_6$:Cr^{3+}.[43,44] It can be noted first of all that the calculated values of $\hbar\omega$(Cu-NH$_3$) and $\hbar\omega$(Cu-Cl) frequencies for the CuCl$_4$(NH$_3$)$_2^{2-}$ center in NH$_4$Cl are in good agreement with the experimental values derived through Raman spectroscopy.[15]

The present calculations lead to a force constant of the axial A_{1g}(Cu^{2+}-X) mode, which is more than three times higher than that corresponding to the A_{1g}(Cu^{2+}-Cl) mode involving equatorial ligands. In particular, the values $K = 13.4$ and 10.9 eV/Å^2 calculated, respectively, for CuCl$_4$(NH$_3$)$_2^{2-}$ and CuCl$_4$(H$_2$O)$_2^{2-}$ in NH$_4$Cl (Table III) are comparable to the stretching A_{1g} force constants derived for systems like CuCl$_4^{2-}$ or CrCl$_6^{3-}$ (Table IV). By contrast, the force constant $K(A_{1g}$;Cu^{2+}-Cl$^-$) = 3.6 eV/Å^2 calculated for the A_{1g}(Cu^{2+}-Cl$^-$) mode of CuCl$_4$(NH$_3$)$_2^{2-}$ is smaller than the figure $K = 4.3$ eV/Å^2 measured for the B_{2g} *bending* mode of CuCl$_4^{2-}$.[38] These results thus stress that in CuCl$_4$X$_2^{2-}$ ($X = $ H$_2$O, NH$_3$) species the bonds in the equatorial plane are much softer than the axial Cu^{2+}-X bonds. This conclusion is supported by the calculated frequencies of both A_{1g}(Cu^{2+}-N) and A_{1g}(Cu^{2+}-Cl$^-$) modes for the CuCl$_4$(NH$_3$)$_2^{2-}$ center.

With regard to the $K(A_{1g}$;Cu^{2+}-Cl$^-$) = 3.44 eV/Å^2 value of the force constant calculated for the CuCl$_4$(H$_2$O)$_2^{2-}$ center in NH$_4$Cl (Table III), it is seemingly similar to that obtained for the CuCl$_4$(NH$_3$)$_2^{2-}$ species. However, it should be noted that the Cu^{2+}-Cl$^-$ distance is *not the same* for both systems.

TABLE IV. Experimental values of vibrational frequencies $\hbar\omega$ (in cm^{-1}) and force constants K (in eV/Å^2) corresponding to two stretching modes (A_{1g} and B_{1g}) and one bending mode (B_{2g}) of the square planar CuCl$_4^{2-}$ unit taken from Ref. [38]. Results for the two stretching modes (A_{1g} and E_g) corresponding to the octahedral CrCl$_6^{3-}$ unit formed in Cs$_2$NaScCl$_6$:Cr^{3+} (Refs. [43] and [44]) are also included together with the equilibrium metal-ligand distance R (in Å) for the two systems.

System	Mode	R	K	$\hbar\omega$
CuCl$_4^{2-}$	A_{1g}	2.26	10	276
	B_{1g}	2.26	5.7	209
	B_{2g}	2.26	4.3	182
CrCl$_6^{3-}$	A_{1g}	2.38	11.7	298
	E_g	2.38	7.4	236

Therefore, if we accept for the equatorial fragment a Grüneisen law

$$\frac{\Delta\omega}{\omega} = -3\gamma\frac{\Delta R_{eq}}{R_{eq}}, \qquad (3)$$

then if $K(A_{1g}$;Cu^{2+}-Cl$^-$) = 3.6 eV/Å^2 for CuCl$_4$(NH$_3$)$_2^{2-}$ ($R_{eq} = 2.78$ Å), we would expect $K(A_{1g}$;Cu^{2+}-Cl$^-$) = 4.8 eV/Å^2 at the calculated value $R_{eq} = 2.70$ Å for CuCl$_4$(H$_2$O)$_2^{2-}$, using a typical value of $\gamma = 2$.[44] However, the calculated $K(A_{1g}$;Cu^{2+}-Cl$^-$) value for CuCl$_4$(H$_2$O)$_2^{2-}$ in Table III is 30% smaller. This result thus stresses that in tetragonal species like CuCl$_4$X$_2^{2-}$ ($X = $ H$_2$O, NH$_3$), it is not correct to treat the axial and equatorial fragments as being independent.[29] Indeed in an a_{1g} bonding or antibonding orbital, a change of the covalency in the equatorial plane modifies that of the axial fragment and vice versa.

The value of the force constant, $K(B_{1g})$, for the stretching B_{1g} mode for a square planar unit is smaller than $K(A_{1g})$ corresponding to the symmetric mode (Table IV). If in a simple model, we accept that the force constant of normal modes depend on both the metal-ligand distance and the distances between adjacent ligand, it turns out that $K(B_{1g})$ only depends on the first variable and for this reason $K(B_{1g}) < K(A_{1g})$. A similar situation holds when comparing the force constants $K(E_g)$ and $K(A_{1g})$ for octahedral units like CrCl$_6^{3-}$.[43,44] Looking at Table IV, it can be seen that the ratio $K(A_{1g})/K(B_{1g})$ is equal to 1.75 for CuCl$_4^{2-}$, while in the case of CrCl$_6^{3-}$ $K(A_{1g})/K(E_g) = 1.6$.

With regard to the calculated force constant for the CuCl$_4$(NH$_3$)$_2^{2-}$ center in NH$_4$Cl, $K(B_{1g}) = 1.3$ eV/Å^2 (Table III), it implies a ratio between $K(A_{1g}$;Cu^{2+}-Cl$^-$) and $K(B_{1g})$ equal to 2.8, which is higher than that measured for CuCl$_4^{2-}$. Moreover, the frequency of this stretching mode is found to be $\hbar\omega(B_{1g}) = 99$ cm^{-1}, which is thus comparable to that of T_{2u} bending modes for octahedral units like CrCl$_6^{3-}$.[43] This fact thus points out that the force constant $K(B_{1g})$ of the CuCl$_4$(NH$_3$)$_2^{2-}$ unit though positive is certainly small for a mode that has a stretching character.

Let us now focus on the comparison between the calculated $K(B_{1g})$ force constant for CuCl$_4$(H$_2$O)$_2^{2-}$ and CuCl$_4$(NH$_3$)$_2^{2-}$ units. On Fig. 3 the ground-state energy dependence on the distortion $Q(B_{1g})$ coordinate for both centers is depicted. Remarkable differences appear when comparing the two curves. Indeed the curve corresponding to
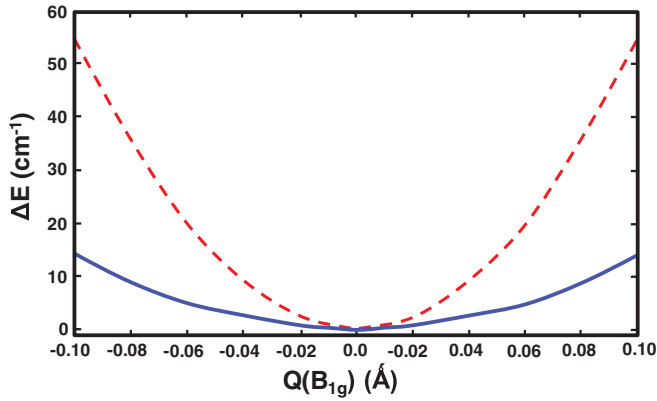
FIG. 3. (Color online) Cross-section of the energy surface along the $Q(B_{1g})$ normal coordinate for small distortions mode. The dashed red and solid blue curves have been calculated, respectively, for $CuCl_4(NH_3)_2^{2-}$ and $CuCl_4(H_2O)_2^{2-}$. Note that the curve for the water-containing unit is almost flat around $Q = 0$.

$CuCl_4(H_2O)_2^{2-}$ is found to be extremely flat with an associated $K(B_{1g})$ force constant, which is *four times* smaller than that obtained for the $CuCl_4(NH_3)_2^{2-}$ and thus nearly equal to zero. Therefore, although the present calculations do not lead to a slightly negative $K(B_{1g})$ value for $CuCl_4(H_2O)_2^{2-}$, they strongly support that the orthorhombic distortion in this unit is much more favorable than for $CuCl_4(NH_3)_2^{2-}$.

D. Vibronic admixture between $a_{1g}^*(\sim 3z^2\text{-}r^2)$ and b_{1g} orbitals

Because the present calculations reproduce the main experimental facts associated with $CuCl_4(NH_3)_2^{2-}$ and $CuCl_4(H_2O)_2^{2-}$ centers, we are now going to focus in studying *why* the $D_{4h} \rightarrow D_{2h}$ instability takes place only in the second system. In order to proceed, we will analyze the main contributions to the vibronic part of the force constant [K_v, see Eq. (1)] associated to the B_{1g} mode.

Let us designate by $H_0(\mathbf{r})$ the adiabatic Hamiltonian, where all nuclei are fixed at equilibrium positions of the electronic ground state whose energy is E_0. In the present cases $H_0(\mathbf{r})$ displays a D_{4h} symmetry. A vibronic interaction, H_v, involving a nondegenerate distortion mode described by a Q coordinate has the form[25]

$$H_v = V'(r)\, Q, \tag{4}$$

where $V'(\mathbf{r})$ and Q belong to the same irreducible representation so that H_v displays the *same* symmetry as $H_0(\mathbf{r})$. If $|\Psi_0\rangle$ means the wave function of the electronic ground state corresponding to the unperturbed Hamiltonian, $H_0(\mathbf{r})$, the inclusion of the vibronic interaction, H_v, induces a change, ΔE_0, on the ground-state energy given by

$$\Delta E_0 = \sum_{n \neq 0} \frac{|\langle \Psi_n | V'(r) | \Psi_0 \rangle|^2}{E_0 - E_n} Q^2, \tag{5}$$

where $|\Psi_n\rangle$ represent excited electronic states of $H_0(\mathbf{r})$. Accordingly, the vibronic admixture of the electronic ground

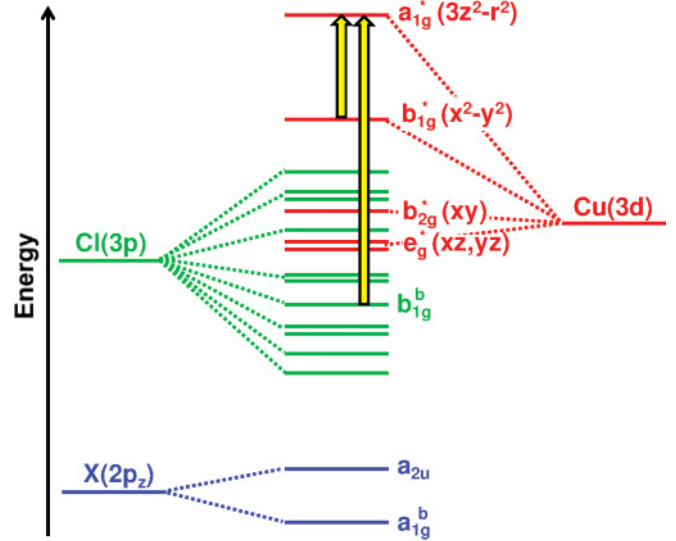FIG. 4. (Color online) Qualitative orbital scheme for $CuCl_4X_2^{2-}$ systems. Mainly $Cu(3d)$, $Cl(3p)$, and $X(2pz)$ levels are represented, respectively, in red (dark gray), green (gray), and blue (medium gray) colors. In the ground-state configuration, all levels are completely filled except for the top a_{1g}^* one. Note that only two b_{1g} levels are present in the scheme, b_{1g}^* and b_{1g}^b, and the $b_{1g}^* \rightarrow a_{1g}^*$ and $b_{1g}^b \rightarrow a_{1g}^*$ excitations leading to the vibronic softening of the B_{1g} vibrational mode are represented by yellow arrows.

state of $H_0(\mathbf{r})$ with excited states leads to a *softening* of the force constant of the Q mode and thus K_v is just given by

$$K_v = 2 \sum_{n \neq 0} \frac{|\langle \Psi_n | V'(r) | \Psi_0 \rangle|^2}{E_n - E_0}. \tag{6}$$

In the present cases both Q and $V'(\mathbf{r})$ transform like B_{1g}. As the electronic ground state belongs to A_{1g}, this means that only the excited states transforming like B_{1g} contribute to K_v.

The electronic configuration of the present Cu^{2+} systems is relatively simple because there is only one unpaired electron in the ground state (Fig. 4). Accordingly, the lowest excited states of this kind of systems just involve the transition of an electron from a fully occupied level to the highest-occupied molecular orbital. This means that we can build B_{1g} excited states transferring the hole in the antibonding $a_{1g}^*(\sim 3z^2\text{-}r^2)$ orbital to b_{1g} orbitals, which are occupied in the ground state.

If we now consider the molecular orbitals of the $CuCl_4X_2^{2-}$ ($X = H_2O$, NH_3) species arising from $3d(Cu)$, $4s(Cu)$, $2p(X)$, and $3p(Cl)$ atomic orbitals (Fig. 4), we realize that there are only *two* orbitals transforming like b_{1g}. One is the antibonding $b_{1g}^*(\sim x^2\text{-}y^2)$ orbital, and the other is the bonding counterpart called b_{1g}^b. Bearing these considerations in mind, the expression of K_v for the present systems can be approximated by

$$K_v = k_v(b_{1g}^*) + k_v(b_{1g}^b), \tag{7}$$

where the two $k_v(b_{1g}^*)$ and $k_v(b_{1g}^b)$ contributions are given by

$$k_v(b_{1g}^*) = 2 \frac{|\langle b_{1g}^* | V'(r) | a_{1g}^* \rangle|^2}{E(b_{1g}^*) - E_0} \tag{8}$$

TABLE V. Values of $\mu(b_{1g}^*)/Q$, $\mu(b_{1g}^b)/Q$, $E(b_{1g}^*)$-E_0, and $E(b_{1g}^b)$-E_0 derived from the present calculations. With these values the contributions to K_v termed $k_v(b_{1g}^*)$ and $k_v(b_{1g}^b)$ have been estimated through Eqs. (8) and (9). The values of $\mu(b_{1g}^*)/Q$ and $\mu(b_{1g}^b)/Q$ are given in Å^{-1}, $E(b_{1g}^*)$-E_0 and $E(b_{1g}^b)$-E_0 are in eV, while $k_v(b_{1g}^*)$ and $k_v(b_{1g}^b)$ are both in eV/Å^2 units.

System	$\mu(b_{1g}^*)/Q$	$E(b_{1g}^*)$-E_0	$k_v(b_{1g}^*)$	$\mu(b_{1g}^b)/Q$	$E(b_{1g}^b)$-E_0	$k_v(b_{1g}^b)$
CuCl$_4$(H$_2$O)$_2^2$	0.7	0.5	0.5	0.65	2.8	2.4
CuCl$_4$(NH$_3$)$_2^{2-}$	0.5	1.1	0.6	0.15	4.9	0.2

$$k_v\left(b_{1g}^b\right) = 2\frac{\left|\langle b_{1g}^b|V'(r)|a_{1g}^*\rangle\right|^2}{E\left(b_{1g}^b\right) - E_0}. \tag{9}$$

Here $E(b_{1g}^*)$-E_0 and $E(b_{1g}^b)$-E_0 are energies of crystal-field and charge-transfer excitations, respectively.

It should be remarked now that a key information on the vibronic matrix elements like $\langle b_{1g}^*|V'(r)|a_{1g}^*\rangle$ or $\langle b_{1g}^b|V'(r)|a_{1g}^*\rangle$ can be derived from the analysis of calculated wave functions for different values of the Q distortion coordinate. In fact, once the path along Q is followed, the a_{1g}^* orbital is transformed into $\widetilde{a_{1g}^*}$ that includes the admixtures with b_{1g}^* and b_{1g}^b

$$|\widetilde{a_{1g}^*}\rangle \cong |a_{1g}^*\rangle + \mu(b_{1g}^*)|b_{1g}^*\rangle + \mu(b_{1g}^b)\left|b_{1g}^b\right\rangle, \tag{10}$$

where $\mu(b_{1g}^*)$ and $\mu(b_{1g}^b)$ do depend linearly on Q and are given by

$$\mu(b_{1g}^*) = Q\frac{\langle b_{1g}^*|V'(r)|a_{1g}^*\rangle}{E(b_{1g}^*) - E_0} \tag{11}$$

$$\mu\left(b_{1g}^b\right) = Q\frac{\langle b_{1g}^b|V'(r)|a_{1g}^*\rangle}{E\left(b_{1g}^b\right) - E_0}. \tag{12}$$

Similarly the wave functions of $\widetilde{b_{1g}^*}$ and $\widetilde{b_{1g}^b}$ orbitals when $Q \neq 0$ are

$$|\widetilde{b_{1g}^*}\rangle \cong |b_{1g}^*\rangle - \mu(b_{1g}^*)|a_{1g}^*\rangle \tag{13}$$

$$\left|\widetilde{b_{1g}^b}\right\rangle \cong \left|b_{1g}^b\right\rangle - \mu(b_{1g}^b)|a_{1g}^*\rangle. \tag{14}$$

Therefore, from the analysis of calculated wave functions for different values of Q, the quantities $\mu(b_{1g}^*)/Q$ and $\mu(b_{1g}^b)/Q$ can *also* be derived. Once these quantities are known, then $k_v(b_{1g}^*)$ and $k_v(b_{1g}^b)$ can be obtained as follows

$$k_v(b_{1g}^*) = 2\left\{\frac{\mu(b_{1g}^*)}{Q}\right\}^2 (E(b_{1g}^*) - E_0) \tag{15}$$

$$k_v\left(b_{1g}^b\right) = 2\left\{\frac{\mu(b_{1g}^b)}{Q}\right\}^2 (E(b_{1g}^b) - E_0). \tag{16}$$

Analyzing the admixture of $|a_{1g}^*\rangle$ into $|b_{1g}^*\rangle$ and $|b_{1g}^b\rangle$ orbitals when the B_{1g} distortion coordinate, Q, is activated, we have derived the values of $\mu(b_{1g}^*)$ and $\mu(b_{1g}^b)$ from the present calculations for different Q values. From them and the knowledge of $E(b_{1g}^*)$-E_0 and $E(b_{1g}^b)$-E_0 excitations from the calculations, a reasonable estimation of $k_v(b_{1g}^*)$ and $k_v(b_{1g}^b)$ contributions can thus be accomplished. Results for both CuCl$_4$(NH$_3$)$_2^{2-}$ and CuCl$_4$(H$_2$O)$_2^{2-}$ centers in NH$_4$Cl are

collected in Table V. It can be noticed that for CuCl$_4$(NH$_3$)$_2^{2-}$ the calculated value of K_v is 0.8 eV/Å^2 and thus smaller than $K(B_{1g}) = 1.3$ eV/Å^2 derived from the *ab initio* calculations. This fact thus supports that the K_v softening induced by the vibronic admixture with B_{1g} excited states is not enough to render the total force constant negative.

By contrast, a quite different situation is found in the CuCl$_4$(H$_2$O)$_2^{2-}$ center, where the $k_v(b_{1g}^b)$ contribution to K_v is found to be about *12 times* higher than in the case of CuCl$_4$(NH$_3$)$_2^{2-}$. Thus, in the case of the CuCl$_4$(H$_2$O)$_2^{2-}$ center, we can understand now that the total force constant of the B_{1g} mode can become slightly negative. It should be noted that the remarkable difference of behavior between CuCl$_4$(H$_2$O)$_2^{2-}$ and CuCl$_4$(NH$_3$)$_2^{2-}$ comes mainly from a $\mu(b_{1g}^b)/Q$ value, which is *four times* higher for the former system than for the latter such as it is shown in Table V. Therefore, this important result underlines that the vibronic coupling of a_{1g}^* with the charge transfer orbital b_{1g}^b is the main source of instability for the CuCl$_4$(H$_2$O)$_2^{2-}$ unit. It should be noted now that if we consider a moderate B_{1g} distortion given by $Q \equiv R_{eq}^l - R_{eq}^s = 0.2$ Å, then the admixture of b_{1g}^b into a_{1g}^* for CuCl$_4$(H$_2$O)$_2^{2-}$ would be *only* around 1% using $\mu(b_{1g}^b)/Q = 0.65$ Å^{-1} (Table V). Similarly, this vibronic coupling decreases the energy of the ground state A_{1g} by only $\sim$0.04 eV, a quantity, which is about 1% of the energy corresponding to a charge-transfer excitation.[15,19] These facts underline that calculations are especially useful for understanding the microscopic origin of phenomena, which can be very subtle.

Looking at Table V, it appears that under the same Q distortion the a_{1g}^* orbital of CuCl$_4$(NH$_3$)$_2^{2-}$ is more reluctant to accept an admixture of an orbital with an equatorial character. This can be related to the axial character of the a_{1g}^* orbital, which is stronger for CuCl$_4$(NH$_3$)$_2^{2-}$ than for CuCl$_4$(H$_2$O)$_2^{2-}$ as shown in Table II.

It is worth noting now that there is some experimental information concerning charge-transfer excitations of CuCl$_4$(NH$_3$)$_2^{2-}$ in NH$_4$Cl. In this case the first allowed charge-transfer excitation corresponds to a $e_u \rightarrow a_{1g}^*$, where e_u is built from equatorial 3p(Cl) orbitals. Such a transition is measured at 4.2 eV,[15,19] which is thus not far from the value $E(b_{1g}^b)-E_0 = 4.9$ eV collected in Table V.

E. Estimation of the orthorhombic distortion for CuCl$_4$(H$_2$O)$_2^{2-}$ in NH$_4$Cl

The present *ab initio* calculations carried out on the CuCl$_4$(H$_2$O)$_2^{2-}$ unit in NH$_4$Cl indicate that this system is in

the verge of the instability although $K(B_{1g})$ is still positive (Table III). A reasonable estimation on the value of the distortion coordinate at equilibrium can, however, be obtained looking at the experimental g tensor and the results embodied in Table V.

Experimental EPR data obtained at $T = 4.2$ K give $g_{xx} = 2.41$ and $g_{yy} = 2.18$.[10] When $T \geqslant 10$ K, the spectrum becomes tetragonal with $\Delta g_{\perp} = (g_{xx} + g_{yy})/2$. For systems with small or moderate covalency, the g-shift arises mainly from the admixture with the lowest excited states due to the spin-orbit coupling.[37] With regard to the difference between g_{xx} and g_{yy}, which is a direct reflect of the orthorhombicity, it can be related to the $\mu(b_{1g}^{*})$ coefficient through the expression

$$g_{xx} - g_{yy} \cong \frac{4\mu(b_{1g}^{*})}{\sqrt{3}} \Delta g_{\perp}. \qquad (17)$$

Using the experimental values obtained for the $CuCl_4(H_2O)_2^{2-}$ unit in NH_4Cl in the preceding formula, it is estimated $\mu(b_{1g}^{*}) = 0.3$. If, according to Table V, $\mu(b_{1g}^{*})/Q = 0.65$ Å^{-1}, then the equilibrium situation for the $CuCl_4(H_2O)_2^{2-}$ unit in NH_4Cl would be given by $Q \equiv R_{eq}^{l} - R_{eq}^{s} = 0.45$ Å. This significant difference between R_{eq}^{l} and R_{eq}^{s} is consistent with the fact that only the superhyperfine interaction with the two Cl^{-} ions involved in the short bond are observed in ENDOR spectra.[10]

It should be noted now that in the case of $Rb_2CuCl_4(H_2O)_2$, the value of $R_{eq}^{l} - R_{eq}^{s}$ is found to be strongly reduced by an applied hydrostatic pressure.[21] In fact, while EXAFS measurements at ambient pressure give $R_{eq}^{l} - R_{eq}^{s} = 0.60 \pm 0.20$ Å, at 15 GPa, the corresponding value is only $R_{eq}^{l} - R_{eq}^{s} = 0.40 \pm 0.20$ Å as a result of the soft character of bonding in the equatorial plane. The estimated value of $R_{eq}^{l} - R_{eq}^{s}$ for the $CuCl_4(H_2O)_2^{2-}$ unit in NH_4Cl is thus not far from the measurements carried out on $Rb_2CuCl_4(H_2O)_2$.

IV. FINAL REMARKS

The present results underline the relevance of *ab initio* calculations for gaining a better insight into the microscopic origin of a subtle phenomenon. From the study carried out in this work, it appears that the orthorhombic instability observed for systems containing the $CuCl_4(H_2O)_2^{2-}$ unit comes mainly from the vibronic admixture of the A_{1g} ground state with a B_{1g} charge-transfer state. This state, which is *not the lowest* one displaying a B_{1g} symmetry, has the unpaired electron in the b_{1g}^{b} orbital made basically of equatorial $3p(Cl)$ orbitals. Similar mechanisms have been shown to be responsible for important structural phase transitions in solids, like ferroelectric and octahedra tilting distortions.[6,7,25]

As a salient feature, the present calculations lead to a value of $\mu(b_{1g}^{b})/Q$ for $CuCl_4(H_2O)_2^{2-}$, which is four times higher than that for the $CuCl_4(NH_3)_2^{2-}$ species, a fact which is behind a much stronger softening of the $K(B_{1g})$ force constant for the former system. As this softening arises mainly from the

vibronic admixture of b_{1g}^{b} into a_{1g}^{*}, the $CuCl_4(H_2O)_2^{2-}$ unit can be viewed as a *model* system for *quantifying* the importance of vibronic coupling in the realm of instabilities.

The present results support that the orthorhombic instability observed for $CuCl_4(H_2O)_2^{2-}$ has nothing to do with what is properly denoted as a Jahn-Teller effect. Indeed this effect requires the existence of an electronic ground state, which is orbitally degenerate in the undistorted configuration. This *restrictive* condition is certainly not fulfilled in the present system where no crossing between B_{1g} and A_{1g} states is accessible for reasonable distortions and where the axial and equatorial force constants are totally different. Furthermore, the distortion due to a true Jahn-Teller effect does not involve the softening of the corresponding force constant, while the present calculations strongly support that this phenomenon takes place in $CuCl_4(H_2O)_2^{2-}$. It is worth noting that the softening of the force constant in cases like $CuCl_4(H_2O)_2^{2-}$ directly reflects the change of the electronic density due to the distortion, a characteristic of all instabilities driven by the so-called pseudo-Jahn-Teller effect.[25] By contrast, that change plays a minor role for understanding the equilibrium geometry and the stabilization energy of systems under a Jahn-Teller effect.[41]

As it has already been pointed out the $D_{4h} \rightarrow D_{2h}$ instability is observed in $CuCl_4(H_2O)_2^{2-}$ embedded as impurity in NH_4Cl[10] and also in the $Rb_2CuCl_4(H_2O)_2$ pure compound, where $CuCl_4(H_2O)_2^{2-}$ units are also well separated.[20,21] This fact underlines that in a pure insulating compound like $Rb_2CuCl_4(H_2O)_2$ the observed orthorhombic distortion has a *local* origin. This conclusion is consistent with the nature of an insulating compound. Indeed, according to Kohn,[45,46] a ground-state wave function in which electrons are *localized* is the fingerprint of every insulating lattice. On the other hand, a structural phase transition requires the existence of a *local* instability with an associated multiwell potential energy, a point that has been stressed by Bruce.[47] According to these ideas, the study of instabilities associated with impurities in insulators can be of help for gaining a better insight into structural phase transitions of pure compounds. Supporting this view in cases like $CuCl_4(H_2O)_2^{2-}$ in NH_4Cl or $BaF_2:Mn^{2+}$, a temperature raising changes abruptly the local symmetry observed experimentally, giving rise to what is called a local phase transition.[10,22,23] A detailed study of this phenomenon observed in $BaF_2:Mn^{2+}$ is reported in Ref. 24.

In conclusion while the calculated energy surfaces for the A_{1g} state in $CuCl_4(H_2O)^{2-}$ in NH_4Cl are certainly flat but do not display a shallow double well, the present results shed light on the subtle origin of the instability observed for this system but not for the $CuCl_4(NH_3)_2^{2-}$ unit. The analysis carried out in this work stresses once more that important variations in the geometrical structure often come from small changes in the electronic levels. Further work on the study of the local origin of phase transitions is now underway.

*garciapa@unican.es

[1] H. W. Jang, A. Kumar, S. Denev, M. D. Biegalski, P. Maksymovych, C. W. Bark, C. T. Nelson, C. M. Folkman, S. H. Baek, N. Balke, C. M. Brooks, D. A. Tenne, D. G. Schlom, L. Q. Chen, X. Q. Pan, S. V. Kalinin, V. Gopalan, and C. B. Eom, Phys. Rev. Lett. **104**, 197601 (2010).

[2] W. Zhong and D. Vanderbilt, Phys. Rev. B **53**, 5047 (1996).

[3] E. Cockayne and B. P. Burton, Phys. Rev. B **62**, 3735 (2000).

[4] K. J. Choi, M. Biegalski, Y. L. Li, A. Sharan, J. Schubert, R. Uecker, P. Reiche, Y. B. Chen, X. Q. Pan, V. Gopalan, L.-Q. Chen, D. G. Schlom, and C. B. Eom, Science **306**, 1005 (2004).

[5] O. Diéguez, S. Tinte, A. Antons, C. Bungaro, J. B. Neaton, K. M. Rabe, and D. Vanderbilt, Phys. Rev. B **69**, 212101 (2004).

[6] P. García-Fernández, J. A. Aramburu, M. T. Barriuso, and M. Moreno, J. Phys. Chem. Lett. **1**, 647 (2010).

[7] P. García-Fernández, J. A. Aramburu, and M. Moreno, Phys. Rev. B **83**, 174406 (2011).

[8] F. Hanic and I. A. Cakajdova, Acta Crystallogr. **11**, 610 (1958).

[9] S. H. Hagen and N. J. Trappeniers, Physica (Utrecht) **47**,165 (1970); Physica (Utrecht) **66**, 166 (1973).

[10] F. Boettcher and J. M. Spaeth, Phys. Status Solidi B **61**, 465 (1974).

[11] M. Moreno, Phys. Status Solidi B **82**, 669 (1977).

[12] M. Riley, M. A. Hitchman, D. Reinen, and G. Steffen, Inorg. Chem. **27**,1924 (1988).

[13] F. Rodríguez, A. G. Breñosa, J. A. Aramburu, M. Moreno, and J. M. Calleja, J. Phys. C **20**, L641 (1987).

[14] J. M. Spaeth and F. Koschnick, J. Phys. Chem. Solids **52**, 1 (1991).

[15] A. G. Breñosa, M. Moreno, F. Rodriguez, and M. Couzi, Phys. Rev. B **44**, 9859 (1991).

[16] G. Steffen, U. Kaschuba, M. A. Hitchman, and D. Reinen, Z. Naturforsch. B **47**, 465 (1992).

[17] A. G. Breñosa, M. Moreno, and J. A. Aramburu, J. Phys. Condens. Matter **3**, 7743 (1991).

[18] J. R. Pilbrow, *Transition Ion Electron Paramagnetic Resonance* (Clarendon Press, Oxford, 1990), p. 291.

[19] J. A. Aramburu and M. Moreno, Phys. Rev. B **56**, 604 (1997).

[20] K. Waizumi, H. Masuda, H. Ohtaki, K. A. Burkov, and L. Chernykh, Acta Crystallogr. Sec. C **48**, 1374 (1992).

[21] F. Aguado, F. Rodríguez, R. Valiente, J. P. Itié, and P. Munsch, Phys. Rev. B **70**, 214104 (2004).

[22] A. G. Badalyan, P. G. Baranov, V. S. Vikhnin, and V. A. Khramtson, JETP Lett. **44**, 110 (1986).

[23] H. Soethe, V. A. Vetrov, and J. M. Spaeth, J. Phys. Condens. Matter **4**, 7927 (1992).

[24] P. García-Fernández, J. A. Aramburu, M. T. Barriuso, and M. Moreno, J. Chem. Phys. **128**, 124513 (2008); J. Phys.: Conf. Ser. **249**, 012033 (2010).

[25] I. B. Bersuker, *The Jahn-Teller Effect* (Cambridge University Press, Cambridge, 2006).

[26] H. Bill, in *The Dynamical Jahn-Teller Effect in Localized Systems*, edited by Yu. E. Perlin and M. Wagner (Elsevier, Amsterdam, 1984), p. 709.

[27] A. Trueba, J. M. Garcia-Lastra, C. De Graaf, P. García-Fernández, J. A. Aramburu, M. T. Barriuso, and M. Moreno, Chem. Phys. Lett. **430**, 51 (2006).

[28] E. Minner, D. Lovy, and H. Bill, J. Chem. Phys. **99**, 6378 (1993).

[29] M. Moreno, M. T. Barriuso, J. A. Aramburu, P. García-Fernández, and J. M. Garcia-Lastra, J. Phys. Condens. Matter **18**, R315 (2006).

[30] D. Ghica, S. V. Nistor, H. Vrielinck, F. Callens, and D. Schoemaker, Phys. Rev. B **70**, 024105 (2004).

[31] P. García-Fernández, J. A. Aramburu, M. T. Barriuso, and M. Moreno, Phys. Rev. B **73**, 184122 (2006).

[32] V. V. Laguta, M. D. Glinchuk, I. P. Bykov, J. Rosa, L. Jastrabík, R. S. Klein, and G. E. Kugel, Phys. Rev. B **52**, 7102 (1995).

[33] A. Trueba, P. García-Fernández, M. T. Barriuso, M. Moreno, and J. A. Aramburu, Phys. Rev. B **80**, 035131 (2009).

[34] G. te Velde, F. M. Bickelhaupt, E. J. Baerends, C. F. Guerra, S. van Gisbergen, J. G. Snijders, and T. Ziegler, J. Comput. Chem. **22**, 931 (2001).

[35] A. D. Becke, J. Chem. Phys. **98**, 5648 (1993).

[36] J. Poater, M. Sola, A. Rimola, L. Rodriguez-Santiago, and M. Sodupe, J. Phys. Chem. A **108**, 6072 (2004).

[37] A. Abragam and B. Bleaney, *Electron Paramagnetic Resonance of Transition Ions* (Claredon Press, Oxford, 1970).

[38] R. G. McDonald and M. A. Hitchman, Inorg. Chem. **25**, 3273 (1986).

[39] P. García-Fernández, A. Trueba, M. T. Barriuso, J. A. Aramburu, and M. Moreno, Phys. Rev. Lett. **104**, 035901 (2010).

[40] M. T. Barriuso, P. García-Fernández, J. A. Aramburu, and M. Moreno, Solid State Commun. **120**, 1 (2001).

[41] P. García-Fernández, I. B. Bersuker, J. A. Aramburu, M. T. Barriuso, and M. Moreno, Phys. Rev. B **71**, 184117 (2005).

[42] C. K. Jørgensen, *Modern Aspects of Ligand Field Theory* (North Holland, Amsterdam, 1971).

[43] O. S. Wenger and H. U. Gudel, J. Chem. Phys. **114**, 5832 (2001).

[44] J. M. García-Lastra, M. Moreno, and M. T. Barriuso, J. Chem. Phys. **128**, 144708 (2008).

[45] W. Kohn, *Many Body Physics* (Gordon and Breach, New York, 1968).

[46] R. Resta, J. Phys. Condens. Matter **14**, R625 (2002).

[47] A. D. Bruce, Adv. Phys. **29**, 111 (1980).